

Intermediate Phase Modulation and Defect Passivation to Stabilize the Photoactive Phase of Formamidinium-Based Perovskites for Air-Ambient Device Fabrication

Nitin Kumar Bansal, Jinyoung Kim, Gyu Min Kim^{b*} and Trilok Singh^{a*}

^aSemiconductor Thin Film and Emerging Photovoltaic Laboratory, Department of Energy Science and Engineering, Indian Institute of Technology Delhi, Hauz Khas, New Delhi 110016, India

^bDepartment of Chemical Engineering, Hankyong National University, 67 Seokjeong-dong, Anseong, Gyeonggi-do 17579, South Korea

Rationale for chain-length selection of alkyl amine additives:

The selection of n-heptylamine (C7) as the amine additive was motivated by the need to balance steric hindrance, molecular mobility, and electronic compatibility during perovskite crystallization. Short-chain alkyl amines (e.g., C4–C5) provide limited steric protection and weaker hydrophobic passivation, resulting in insufficient suppression of defect formation. In contrast, longer alkyl chains (\geq C8) tend to introduce excessive insulating character, which can impede charge transport and disrupt crystallization continuity. A C7 alkyl chain offers an optimal compromise, enabling effective coordination of the terminal $-\text{NH}_2$ group with Pb^{2+} ions while maintaining favorable film morphology, crystallization kinetics, and interfacial stability, as supported by previous reports on alkyl amine and spacer-assisted perovskite growth.¹⁻³

Table: S1 Circuit fitting parameters of TRPL for carrier life time calculation.

Specification	D ₁ (%)	τ_1 (ns)	D ₂ (%)	τ_2 (ns)	τ_{avg} (ns)
CB	72	98.5	28	670.3	259.13
n-HA + CB	38	285.7	62	1125.6	814.40

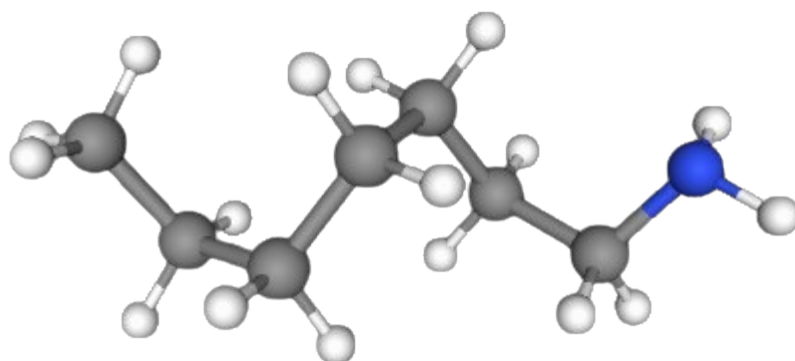


Figure S1: Schematic illustration of the molecular structure of *n*-heptylamine (*n*-HA), highlighting the terminal amine group and the linear C7 alkyl chain

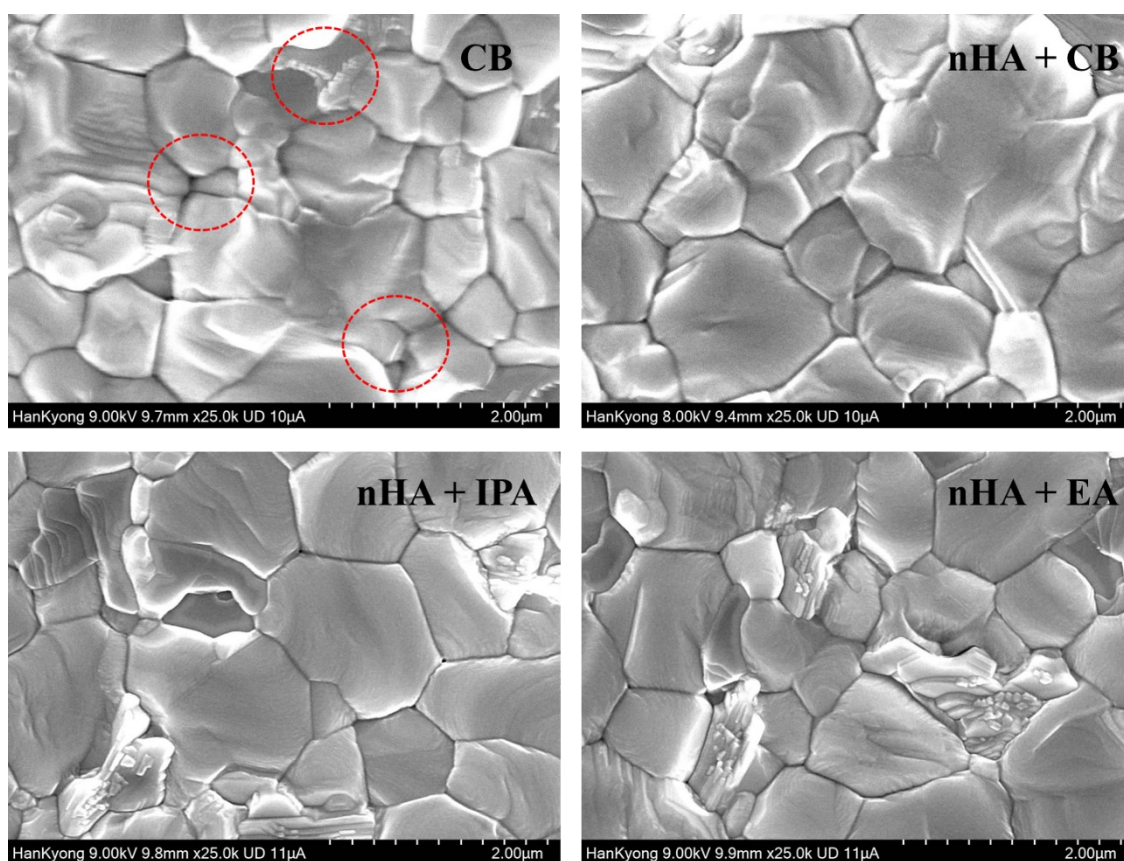


Figure S2: Top view SEM of perovskite films with various antisolvent combinations.

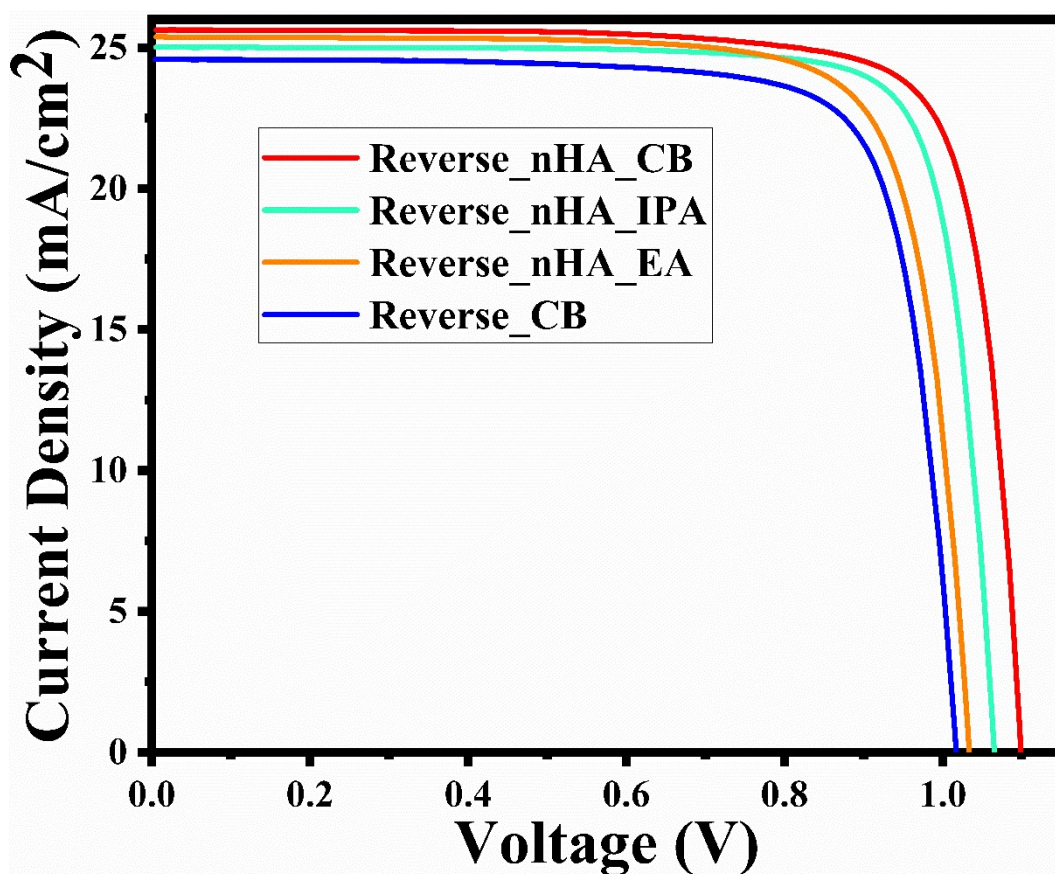


Figure S3: Reverse scan JV curves for various antisolvent combinations.

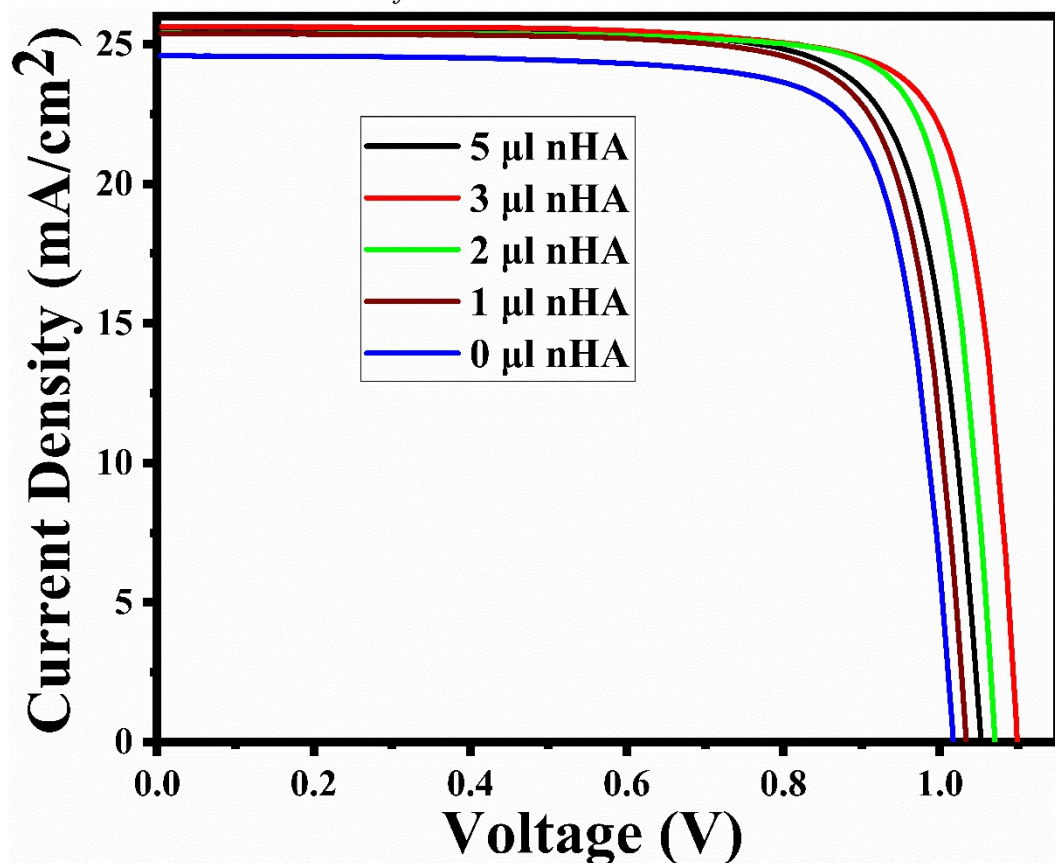


Figure S4: Concentration optimization of n-HA mixed in CB as antisolvent.

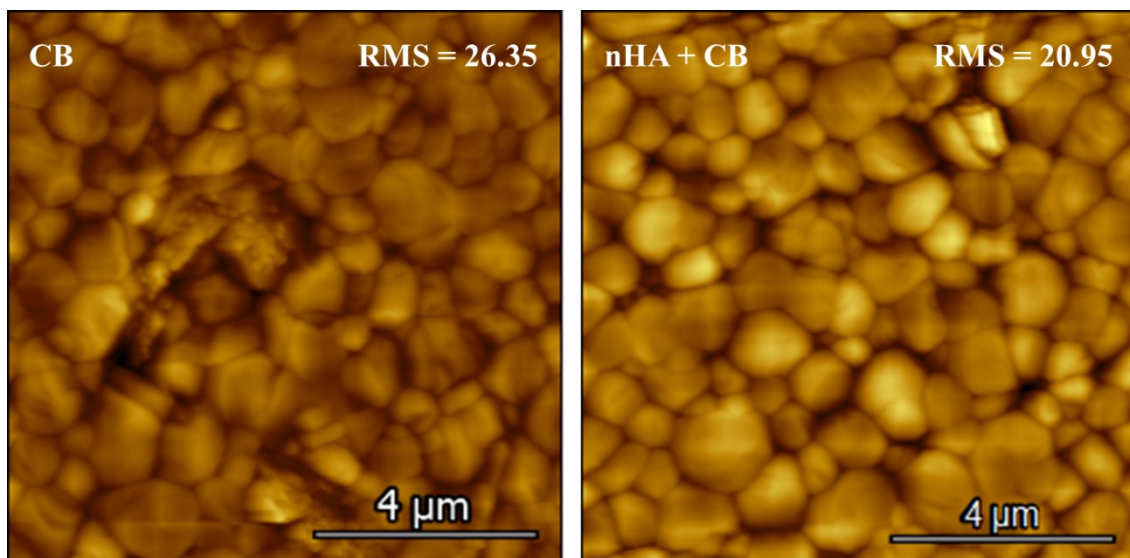


Figure S5: AFM of pristine and modified perovskite films.

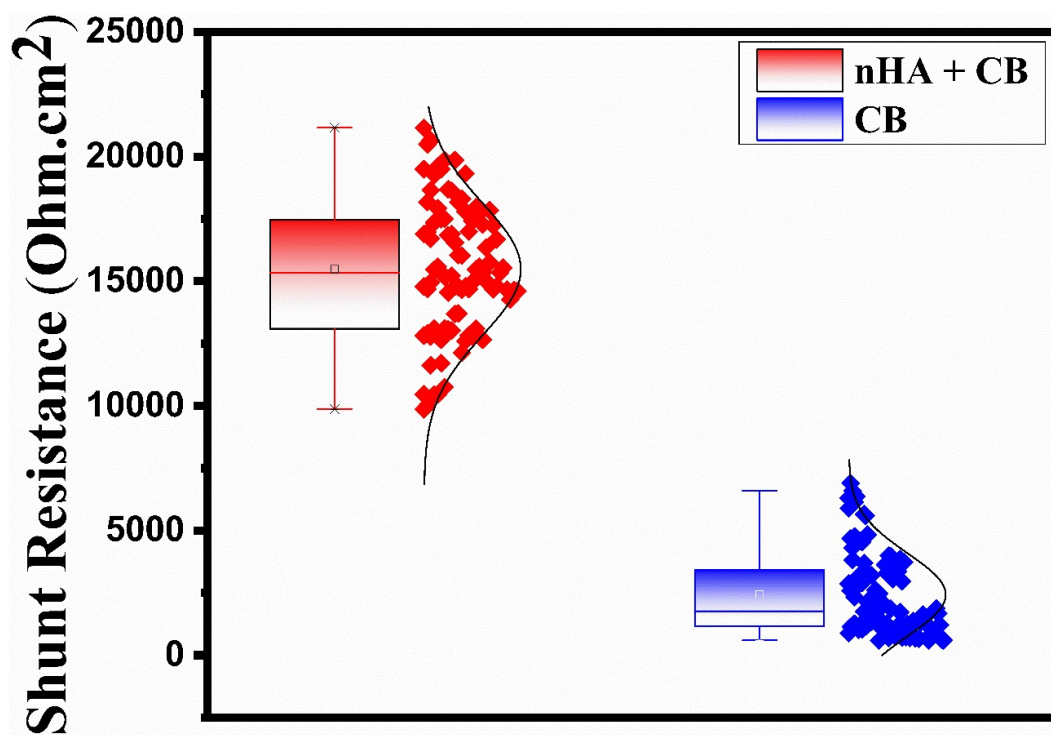


Figure S6: Effect of modification on the distribution of shunt resistance.

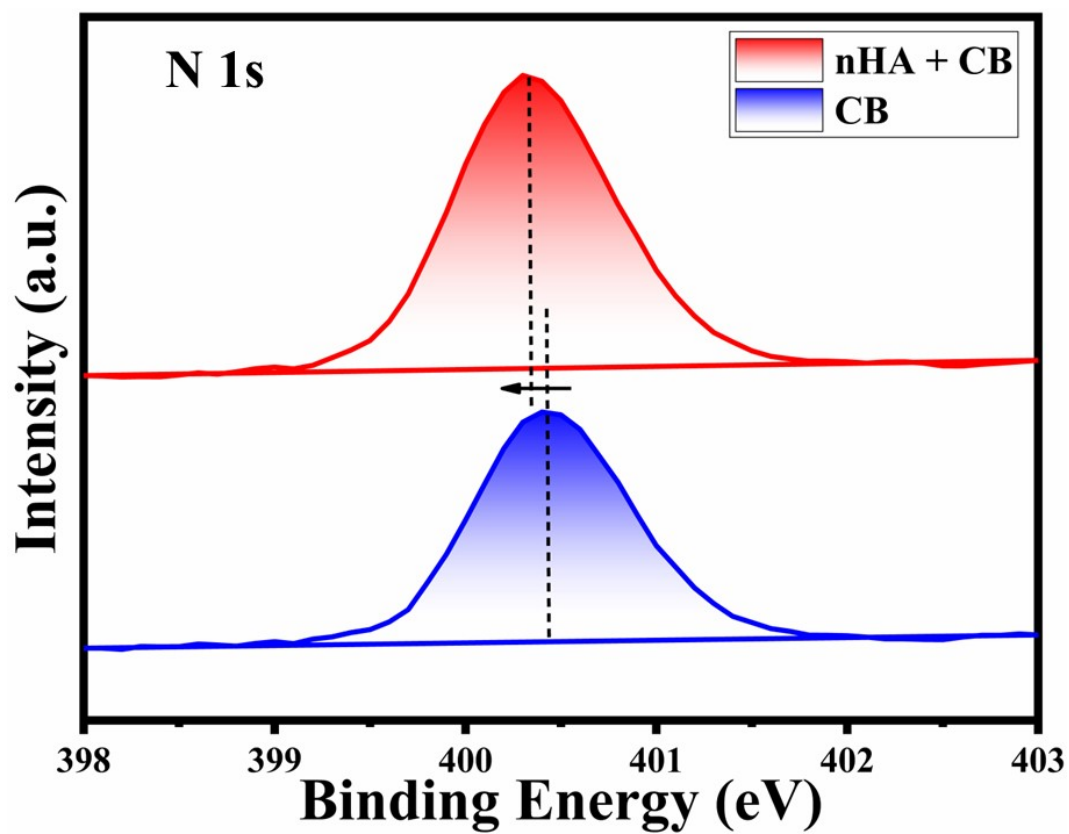


Figure S7: N1s peak of perovskite film from XPS elemental analysis.

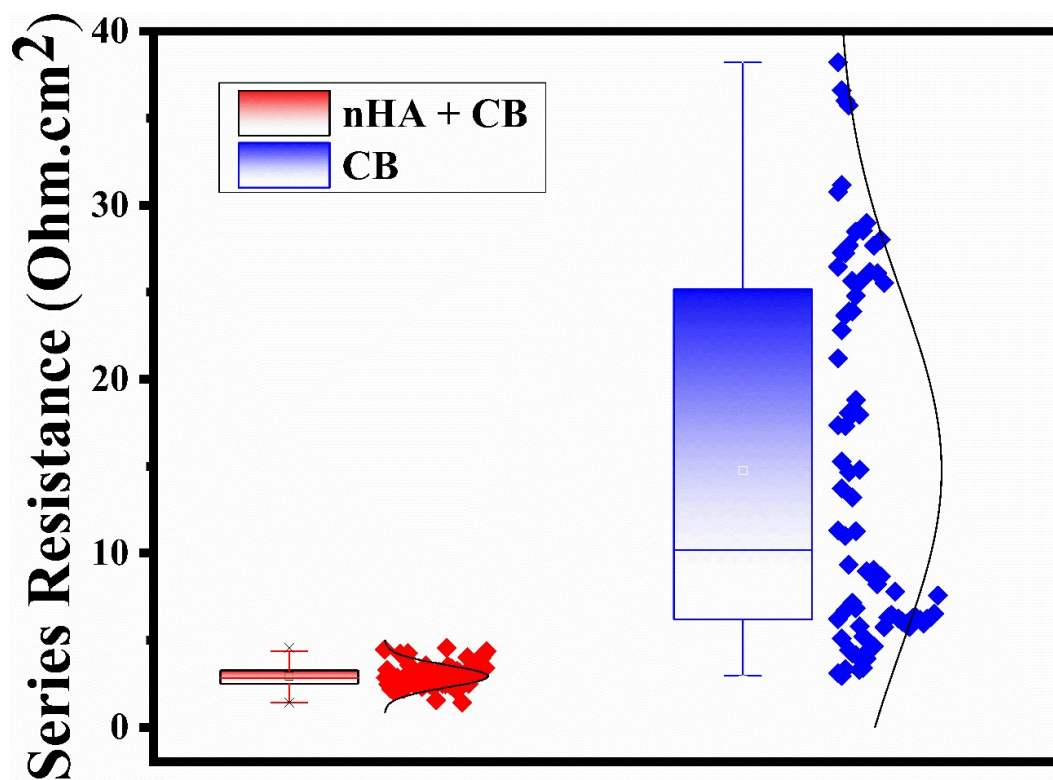


Figure S8: Effect of modification on the distribution of series resistance of devices.

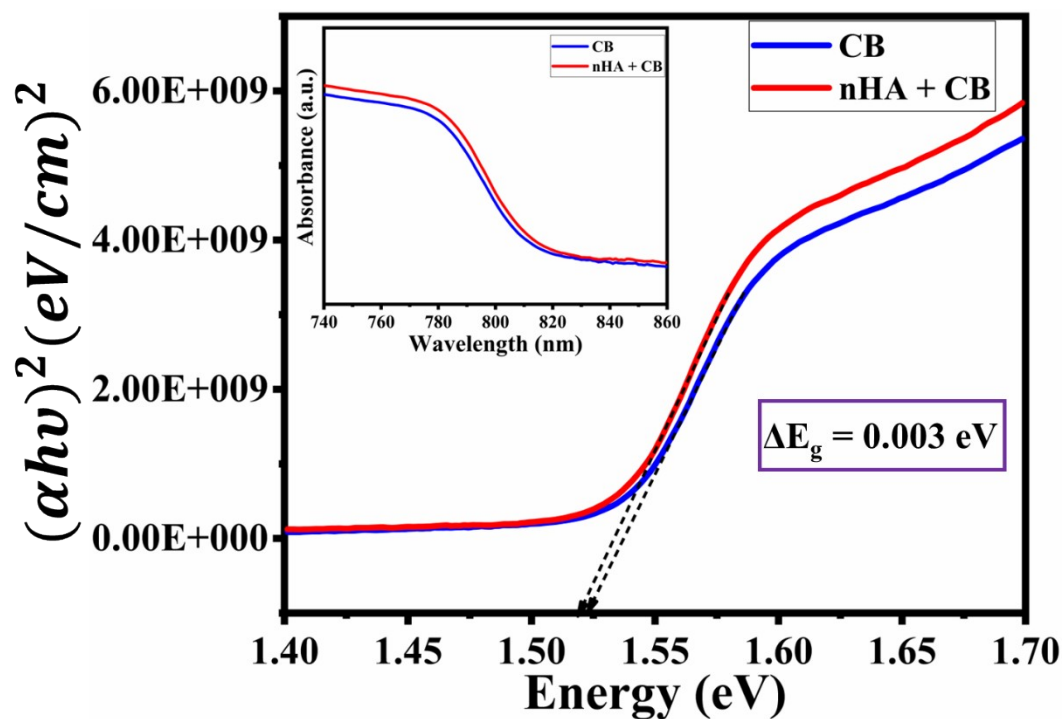


Figure S9: Tauc plot analysis of pristine and modified perovskite films (Inset: UV-Vis absorbance spectra of perovskite films).

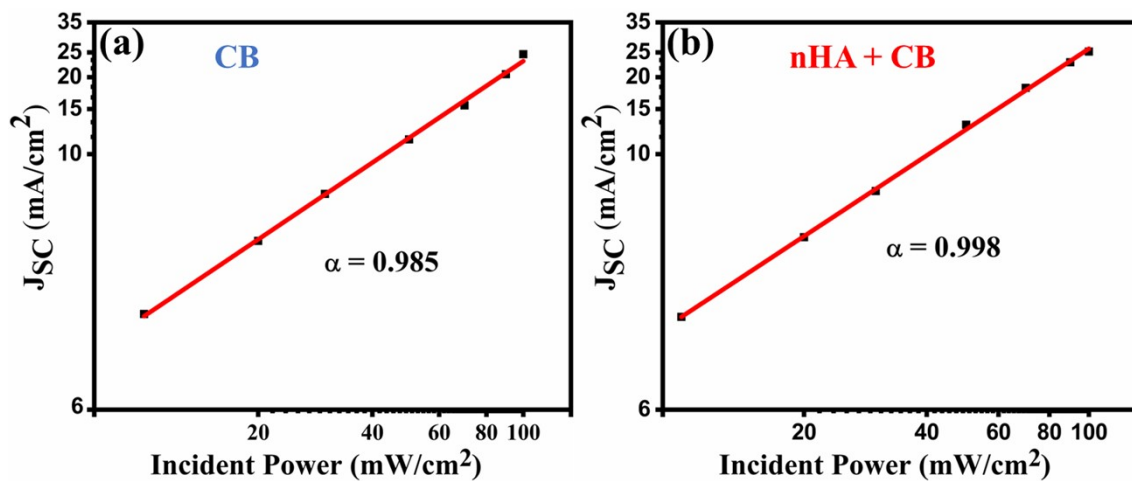


Figure S10: Light intensity-dependent variation of short circuit current at log-log scale.

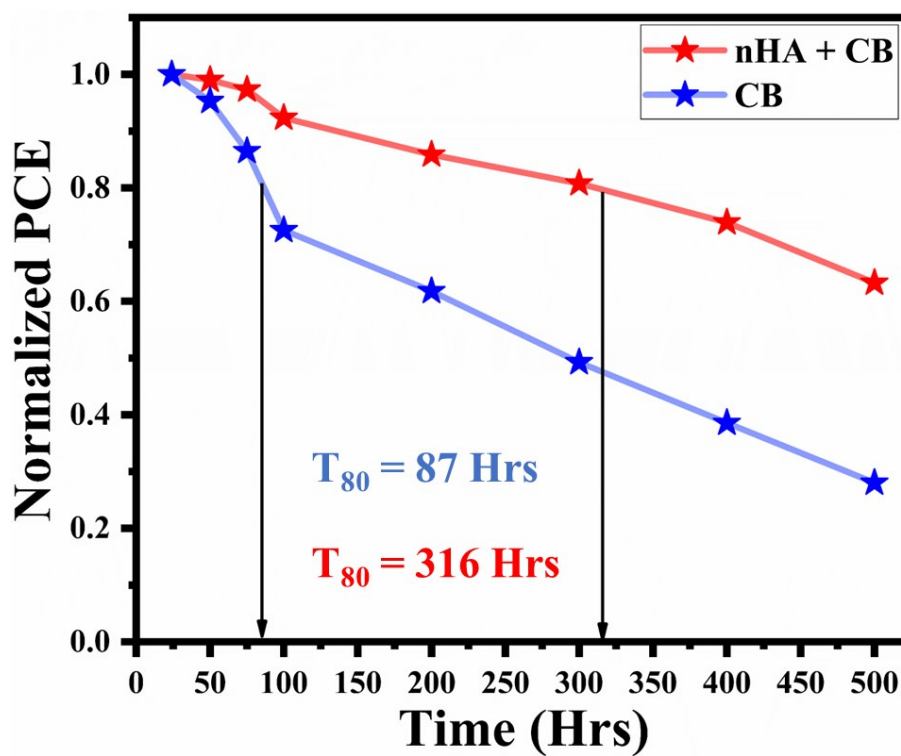


Figure S11: Stability analysis of perovskite devices at the elevated humidity value.

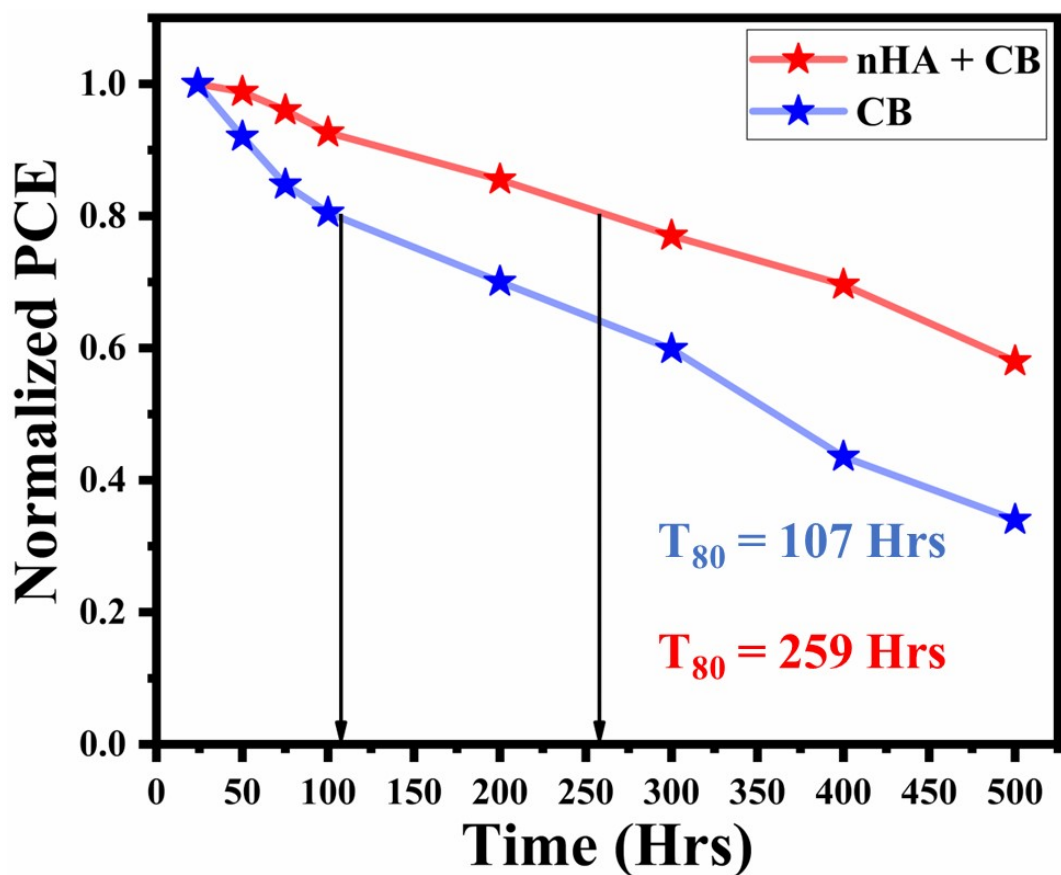


Figure S12: Stability analysis of perovskite devices at the elevated temperature value.

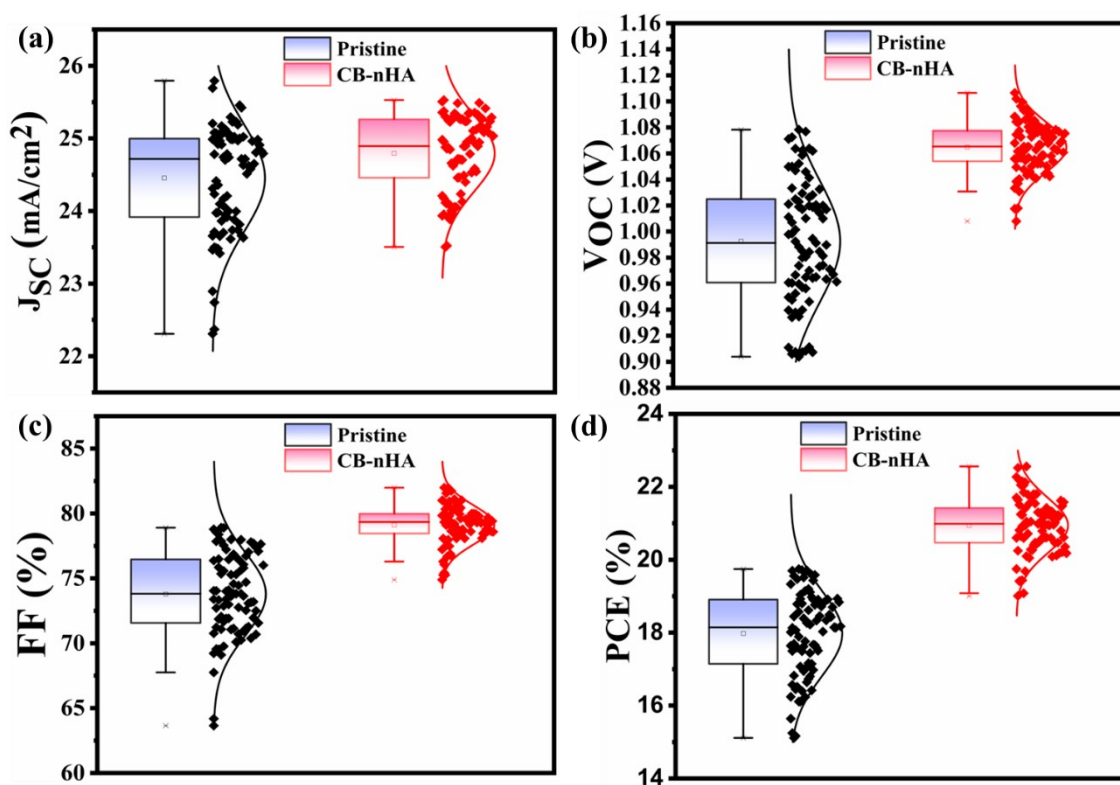


Figure S13: Distribution of performance parameters for pristine and modified devices.

References:

1. H. Nagasaka, M. Yoshizawa-Fujita, Y. Takeoka and M. Rikukawa, *ACS Omega*, 2018, **3**, 18925-18929.
2. Y. Tezuka, K. Umemoto, M. Takeda, Y. Takahashi, H. Ebe, J. Enomoto, S. Rodbuntum, T. Nohara, D. Fontecha, S. Asakura, T. Chiba, M. I. Furis, T. Yoshida, H. Uji-i and A. Masuhara, *Japanese Journal of Applied Physics*, 2020, **59**, SDDC04.
3. P. Zhao, J. Subbiah, B. Zhang, J. A. Hutchison, G. Ahluwalia, V. Mitchell, K. P. Ghiggino and D. J. Jones, *Advanced Materials Interfaces*, 2023, **10**, 2202313.